

Article

A Rapid Label-Free Fluorescent Aptasensor PicoGreen-Based Strategy for Aflatoxin B₁ Detection in Traditional Chinese Medicines

Cheng Zhang^{1,2}, Xiaowen Dou¹, Lei Zhang¹, Meifeng Sun^{1,2}, Ming Zhao², Zhen OuYang², Dandan Kong¹, F. Logrieco Antonio³ and Meihua Yang^{1,*}

¹ Key Laboratory of Bioactive Substances and Resources Utilization of Chinese Herbal Medicine, Ministry of Education, Institute of Medicinal Plant Development, Chinese Academy of Medical Sciences, Peking Union Medical College, Beijing 100193, China; zcmcotoxin@163.com (C.Z.); douxiaowen573@163.com (X.D.); zhanglei-85@163.com (L.Z.); Marksmf@163.com (M.S.); k_dandan@163.com (D.K.)

² School of Pharmacy JiangSu University, Zhenjiang 212013, China; yxzm@ujs.edu.cn (M.Z.); zhenouyang@ujs.edu.cn (Z.O.Y.)

³ National Research Council of Italy, CNR-ISPA, Via G. Amendola, 122/O, I-70126 Bari, Italy; antonio.logrieco@ispa.cnr.it

* Correspondence: yangmeihua15@hotmail.com.; Tel.: +86-010-5783-3277

Received: 8 January 2018; Accepted: 26 February 2018; Published: 28 February 2018

Abstract: Aflatoxin B₁ (AFB₁) is a very hazardous carcinogen, readily contaminating foodstuffs and traditional Chinese medicines (TCMs) that has inspired increasing health concerns due to dietary exposure. Colloidal nanocrystals have been proposed as optical labels for aptasensor assembly, but these typically require tedious multistep conjugation and suffer from unsatisfactory robustness when used for complex matrices. In the present study, we report a rapid and sensitive method for screening for trace AFB₁ levels in TCMs using a label-free fluorescent aptasensor PicoGreen dye-based strategy. Using PicoGreen to selectively measure complementary double-stranded DNA, fluorescence enhancement due to dsDNA is ‘turned off’ in the presence of AFB₁ due binding of aptamer target over complementary sequence. Self-assembly of a label-free fluorescent aptasensor based on AFB₁ aptamer and PicoGreen dye was performed. Due to competition between the complementary sequence and AFB₁ target, this rapid method was capable of highly sensitive and selective screening for AFB₁ in five types of TCMs. This proposed approach had a limit of detection as low as 0.1 µg·L⁻¹ and good linearity with a range of 0.1–10 µg·L⁻¹ (0.1–10 ppb). Among the 20 samples tested, 6 batches were found to be contaminated with AFB₁ using this method, which was confirmed using sophisticated liquid chromatography-electrospray ionization-tandem mass spectrometry/mass spectrometry analysis. The results of this study indicate the developed method has the potential to be a simple, quick, and sensitive tool for detecting AFB₁ in TCMs.

Keywords: aflatoxin B₁; aptamer; PicoGreen; fluorescence; traditional Chinese medicines

Key contribution: A rapid label-free fluorescent aptasensor PicoGreen-based strategy was proposed to screen for AFB₁. This rapid method had good sensitivity and selectivity; making it a potential tool for detecting AFB₁ in traditional Chinese medicines; such as in areca nuts.

1. Introduction

Aflatoxins, primarily produced by *Aspergillus flavus* and *A. parasiticus*, were defined as Group 1 human carcinogens by the International Agency for Research on Cancer in 1993 [1]. Highly lipophilic mycotoxins, aflatoxins can be quickly absorbed in the alimentary canal. It is estimated that 55 million of

people worldwide have been exposed in an uncontrolled manner to aflatoxins through their diet [2,3]. In addition, aflatoxins can enter the bloodstream directly through inhalation [4]. There has been an increasing incidence of hepatomas associated with aflatoxin B₁ (AFB₁) that has been inspiring significant concern. AFB₁ has been shown to have a variety of biological activities, including causing acute toxicity, stunting growth, being teratogenic, mutagenic, immunosuppressive, and genotoxic, and damaging membranes by increasing lipid peroxidation and generation of free radicals [5–7]. In view of the serious effects on humans of and pollution risk by this mycotoxin, governments and related organizations have established strict regulations and detection methods to limit aflatoxin levels in foodstuffs.

Currently, there is a range of methods available for detecting aflatoxins. These methods typically involve thin layer chromatography [8], high performance liquid chromatography (HPLC) coupled to fluorescent detectors [9], liquid chromatography coupled to mass spectrometry (MS) [10,11], and enzyme-linked immunosorbent assays (ELISA) [12]. However, the thin layer chromatography method is cumbersome, has low sensitivity, and requires a large amount of organic reagent. High performance liquid chromatography coupled to fluorescent detectors and liquid chromatography coupled to mass spectrometry rely on pre- or post-derivatization and a sophisticated mass spectrometer prior for detection, respectively. In addition, these methods require tedious pretreatments, making screening more difficult and increasing analysis time. Despite the rapidity and simplicity of classical enzyme-linked immunosorbent assays, these can have false positive results, large deviations in qualitative results, and matrix interference [13–15]. Antibody-based bioanalysis to detect contaminants requires laborious, expensive, and time-consuming antibody preparation and may be susceptible to problems with stability or modification. Therefore, rapid, simple, sensitive, and cost-effective methods are highly desired for quantifying AFB₁ levels in matrices, including traditional Chinese medicines (TCMs).

To overcome the above limitations, aptamers (Apt) have been developed as novel recognition molecules promising for use in analytical applications [16]. Aptamers are single-stranded DNA or RNA molecules that can bind with high affinity and specificity to various target ligands, including small-molecule drugs, peptides, proteins, and cells. These molecules are selected *in vitro* using systematic evolution of ligands by exponential enrichment [17,18]. In addition to their strong target-binding ability, aptamers offer several notable advantages over traditional protein antibodies, including target diversity, high stability, and easy synthesis and modification for applications [19,20]. A variety of aptamer-based analytical techniques have been developed, including colorimetric assays, fluorescence assays, and electrochemical aptasensor methods [21]. Fluorescence-based analysis is particularly appealing due to its high sensitivity and the variety of flexible platforms available [22–27]. These fluorescence platforms can be categorized into those involving labeled [27] and label-free aptasensors [24]. Labeled aptasensors have good stability, low limits of detection, and wide detection ranges. However, these molecules are also complicated to couple, difficult to purify, and not conducive to rapid detection. By contrast, label-free aptasensor strategies have garnered much attention due to not requiring complex coupling steps, having stable signals and low matrix interference, and the capacity for use in rapid detection.

In this present study, we developed a facile and label-free aptasensor strategy for highly sensitive and selective fluorescence detection of AFB₁ using commercially available PicoGreen (PG). Briefly, the fluorescent signal of PG generated upon binding to double-stranded DNA (dsDNA) formed from an aptamer and its complementary sequence (Seq) was turned off in the presence of AFB₁ due to AFB₁ recognition by the aptamer prior to the Seq. This assay had high sensitivity and has great potential for use for on-site and rapid analysis, which is conducive to detecting mycotoxins in TCMs.

2. Results and Discussion

2.1. Principle Underlying Label-Free Aptasensor Strategy

PG reagent is an asymmetric cyanine dye that alone does not fluoresce. However, after binding to dsDNA, the fluorescence of this dye increases by more than 1000-fold [28]. A sensitive and quantitative probe, this commercially available dye allows for the detection of dsDNA levels as low as 25 ng L⁻¹. Utilizing PG's excellent selectivity and sensitivity for trace dsDNA, a rapid and straightforward label-free aptasensor strategy based on competitive recognition of aptamer by AFB₁ and single-stranded DNA (ssDNA) was proposed for small target screening. The sensing mechanism of the proposed method is illustrated in Figure 1. In the control group, Seq hybridized with free AFB₁-specific aptamer. After the formation of dsDNA, PG inserts into the minor groove of the dsDNA duplex, resulting in significant enhancement of fluorescence [29]. In the test group, AFB₁ bound to aptamer prior to dsDNA formation, leaving only a small amount of aptamer remaining for Seq to react with, thus causing a decrease in PG fluorescence intensity compared to the control group. Based on this decrease in fluorescence intensity, AFB₁ could be quantified. Importantly, a critical precondition of this methodology is the fluorescent intensity could not be increased by the targets, Seq, or aptamer. This was examined and the results are presented in Figure 2. The blank solution produced negligible fluorescence, while the aptamer and Seq each exhibited very weak fluorescence, likely from the presence of dsDNA duplexes within regions of the ssDNA. As shown in Figure 2, when both aptamer and Seq were present in solution, there was a strong fluorescent signal. Upon addition of the target, this fluorescence dramatically decreased in intensity. This phenomenon was perfectly in line with our hypothesis. In the presence of AFB₁, AFB₁ bound to the aptamer in advance of the complementary sequence, greatly reducing the chance of dsDNA formation and leading to a decrease in fluorescence. To further validate the proposed method, a mismatch experiment was conducted, and the results are presented in Figure S1. In this experiment, Apt1 recognized AFB₁ and was used in the mismatch test. Various concentrations of AFB₁ were mixed with Apt1, then identical amounts of Seq1, 2, and 6 (a total of 80 bases) were individually added to the above mixture and the intensity of each well was recorded. Apt1 and Seq1 sequences were completely complementary, while Seq2 and 6 were only partially complementary to Apt1. Fluorescence in the Apt1+Seq1 group decreased gradually as AFB₁ content increased, while Apt1+Seq2 and Apt1+Seq6 caused irregular and negligible changes in fluorescence intensity. These results support that the proposed label-free aptasensor strategy is promising for quantitative analysis and effective and suitable for AFB₁ detection.

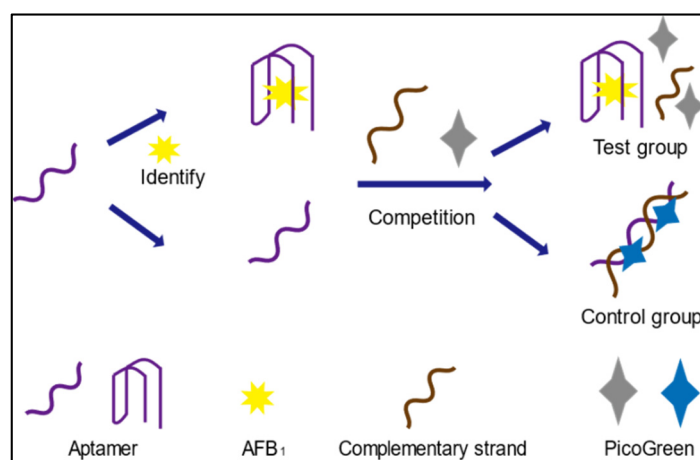


Figure 1. Schematic illustration of fluorescent detection of AFB₁ by a label-free aptasensor.

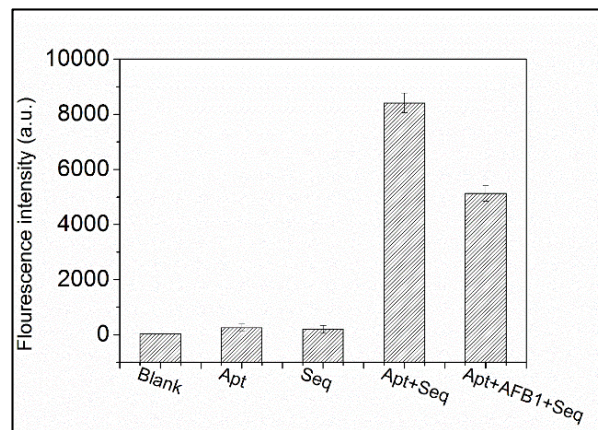


Figure 2. Principle of the label-free fluorescent aptasensor strategy of AFB₁ detection. Results from three independent experiments.

2.2. Screening of AFB₁-Specific Aptamers Using Aptasensor Strategy

Affinity and selectivity are bioanalysis foundations. In recent years, a number of aptamers have been selected for AFB₁ recognition. Therefore, a total of seven aptamers (list in the Table 1) against AFB₁ previously reported in the literature, as well as commonly used and patented sequences relating to selection or affinity studies, were investigated in this study. Aptamers have been described with defined dissociation constants (K_ds). While K_d can be used to identify strong binding between aptamers and a small target, it fails to accurately describe specificity and cross-reactivity. Therefore, we used a simple and rapid method to screen for suitable aptamers using a commercial fluorescent dye. The results are shown in Figure 3. Compared with the corresponding control groups, the test groups containing AFB₁ and Apt1, 2, 5, 6, and 7 had significantly less fluorescence intensity, indicating these aptamers strongly and selectively bound to AFB₁ under these conditions. In particular, Apt5 bound the strongest with a distinct fluorescence intensity difference value (ΔF) of 3488.85 a.u. While Apt3 and 4 had good selectivity toward AFB₁, neither displayed a decrease in fluorescence during the experiment in this study. Based on the notable difference in fluorescence intensity, Apt5 was used with non-labeled fluorescent dye PG to detect dsDNA.

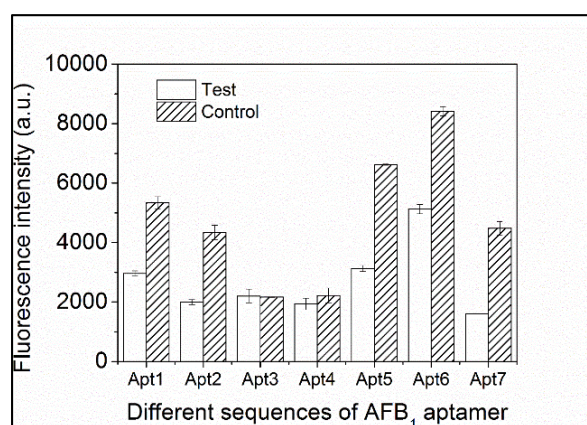


Figure 3. Evaluation of selectivity of aptasensor for AFB₁ (using aptamers with different sequences).

Table 1. DNA aptamer used in this study.

NO.	Sequence (5'–3')	References
Apt 1	AGCAGCACAGAGGTCAGATGGTGCTATCATGCGCTCAATGGGAGACTT TAGCTGCCCCACCTATGCGTGCTACCGTGAA	[30]
Apt 2	AGCAGCACAGAGGTCAGATGTCTAAATGACACCTTTTCAACCTACTGA CTTGGTTACTACCTATGCGTGCTACCGTGAA	[30]
Apt 3	GTTGGGCACGTGTTGTCTCTGTGTCTCGTGCCCTTCGCTAGGCCACA	[31]
Apt 4	AAAGTTGGGCACGTGTTGTCTCTGTGTCTCGTGCCCTTCGCTAGGCC ACAAAAA	[32]
Apt 5	CAGCTTATTCAATTGTGCAGGGGGAGGGGAGTGGTGGCTCGCGGTGC GTGGTGGCTGTAGATAGTAAGTGCAATCTA	[33]
Apt 6	GCATCACTACAGTCATTACGCATCGGGTAATCCTAAGCGGAAGTGGG AGTGGGAGGTAATCGTGTGAAGTGCTGTCCC	[34]
Apt 7	TTTTTTGTTGGGCACGTGTTGTCTCTGTGTCTCGTGCCCTTCGCTAGGC CCAC	[35]

2.3. Specificity of the Label-Free Fluorescent Aptasensor for AFB₁

The specificity of this assay for AFB₁ and its analogues, aflatoxin M₁ (AFM₁), ochratoxin A (OTA), zearalenone (ZEN), fumonisin B₁ (FB₁), and deoxynivalenol (DON), was assessed using the proposed aptasensor strategy. As shown in Figure 4A, cross-reactivity was evaluated with 5 μg·L⁻¹ of the aforementioned mycotoxins. AFB₁ had the highest ΔF, while the other five analogues had a low ΔF, when detected with Apt5. This indicated Apt5 bound to AFB₁ the strongest and had only slight binding with other mycotoxins. In particular, AFM₁ contains a carbon skeleton identical to that in AFB₁ except for a hydroxyl group on a C atom. However, the ΔF of AFB₁ was still up to five-fold higher than that of AFM₁ when using Apt5 as the recognition sequence. Based on these results, the other four aptamers tested (Apt1, 2, 6, and 7) were also able to recognize AFB₁, but had much poorer specificity than Apt5. For example, the ΔF for Apt7 obtained for the six tested mycotoxins were almost identical. Moreover, as shown in Figure 4B, when AFB₁ existed in the mixed standard solution, the fluorescence intensity decreased with increasing in concentration of AFB₁. On the contrary, the variation was not obvious. For trace detection methods, significant cross-reaction can limit practical applications. In order for our assay to be sensitive enough to detect AFB₁ in TCMs, Apt5 was used in follow-up experiments.

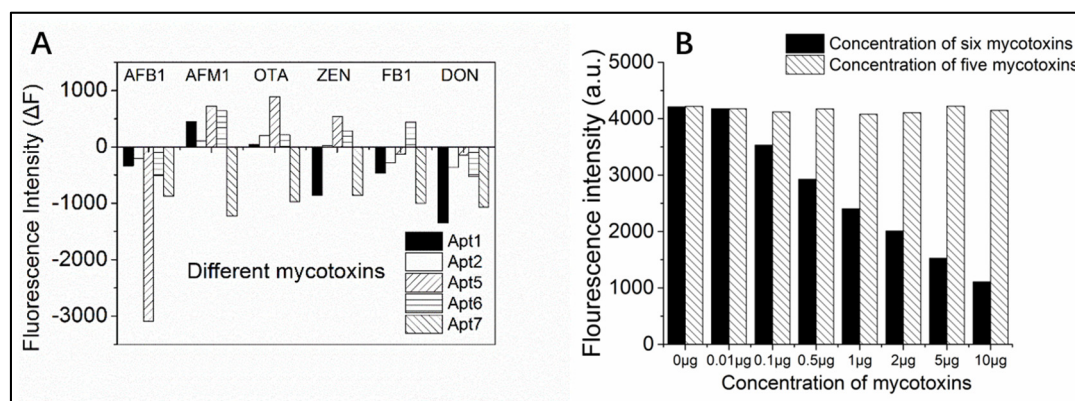


Figure 4. Label-free aptasensor using PG for detection of AFB₁. (A) Evaluation of aptasensor specificity for AFB₁ compared to AFM₁, OTA, ZEN, FB₁, and DON; (B) evaluation of aptasensor specificity for AFB₁ in mixed standard solution (the black bar contained AFB₁, another bar without AFB₁).

2.4. Optimization of Detection Conditions

2.4.1. PG Amount

The assay established in this study was based on a combination of fluorescent dye and dsDNA. Therefore, the amount of fluorescent dye used is an important parameter in detection performance. Different PG solution amounts (5, 10, 15, 20, and 25 μL) were introduced to the mixture of Apt and Seq. As shown in Figure S2, the fluorescence intensity was directly correlated with PG, peaking when 15 μL PG was added. Under a constant quantity of Apt and Seq, increasing the PG did not lead to an intensity increase, supporting that 15 μL PG was enough to mark dsDNA after binding of complementary strands.

2.4.2. PG and dsDNA Reaction Time

Our approach relies on changes in PG fluorescence intensity in response to competitive binding to Apt between Seq and AFB₁. AFB₁ had priority for binding to Apt, while the subsequent Seq probably competitively combined with Apt from the Apt-AFB₁ adduct during the reaction time. Therefore, it is important to determine the optimal time for dsDNA formation and PG labeling. As shown in Figure S3, the intensities for all AFB₁ concentrations first increased and then decreased as the reaction time was extended up to 30 min, suggesting there was competition for Apt between Apt-AFB₁ adduct and Apt-Seq duplex. Interestingly, in contrast to our previous assumption, at the beginning of the 5 min reaction, Apt-Seq duplex formed from competition with Apt-AFB₁ complex based on ascending signal. Then the Apt separated from the dsDNA duplex and formed Apt-AFB₁ complex, gradually leading to a decrease in fluorescence after 5 min. Moreover, signals after a 5 min reaction were distinct for different concentrations of AFB₁, demonstrating a linear relationship between AFB₁ concentration and intensity change. Therefore, a 5 min reaction time was chosen for PG fluorescent dye and dsDNA.

2.5. Method Validation

Prior to quantitative analysis of AFB₁ in real samples, detection in the presence of matrix interference was examined. A preliminary study was conducted where undiluted primary negative extract in Tris-EDTA (TE) buffer (10 mM Tris-HCl and 1 mM EDTA-2Na, pH 8.0) was mixed with a series of AFB₁ standard solutions and fluorescence was measured at 520 nm. As shown in Figure S4, areca nut extract containing various levels of AFB₁ displayed a negligible decrease in signal compared to the blank extract, but incurred high background levels. Based on this, various AFB₁ levels in primary extract and TE buffer were screened using the proposed method. As observed in Figure S4, in comparison with TE buffer, TCMs extract had high background fluorescence, but this background did not obscure the decrease in signal as AFB₁ levels increased. To deal with the complicated matrix, an approach combining dissolution in TE buffer and background correction was adopted.

Under the optimal conditions, various concentrations of AFB₁ were detected using the proposed method. As shown in Figure 5, the fluorescence intensity of PG decreased gradually as AFB₁ concentrations in the reaction system increased. A good linear relationship between the fluorescence intensity (y) and the logarithm of the concentration ($\text{Lg}x$) with a correlation coefficient of 0.9905–0.9976 was observed. The linear range was 0.1–10 $\mu\text{g}\cdot\text{L}^{-1}$ (0.1–10 ppb). We defined 10% fluorescence inhibition as the lowest detected concentration, thus allowing a limit of detection (LOD) of 0.1 $\mu\text{g}\cdot\text{L}^{-1}$ (coefficient of variation, CV < 2%). This suggests the AFB₁-binding aptamer in the present study allowed for quantitative detection of AFB₁ for levels as low as 0.1 $\mu\text{g}\cdot\text{L}^{-1}$. Recovery assays were performed where reactions were spiked with three AFB₁ concentrations, 2.5, 5, and 10 $\mu\text{g}\cdot\text{kg}^{-1}$, which resulted in recoveries of 71.1–99.2, 78.5–100.9, and 79.4–100.4%, respectively (Table 2). Analyses were performed in triplicate. Good reproducibility was observed with reproducibility standard deviations of 2.6–10.2%, which are within acceptable levels.

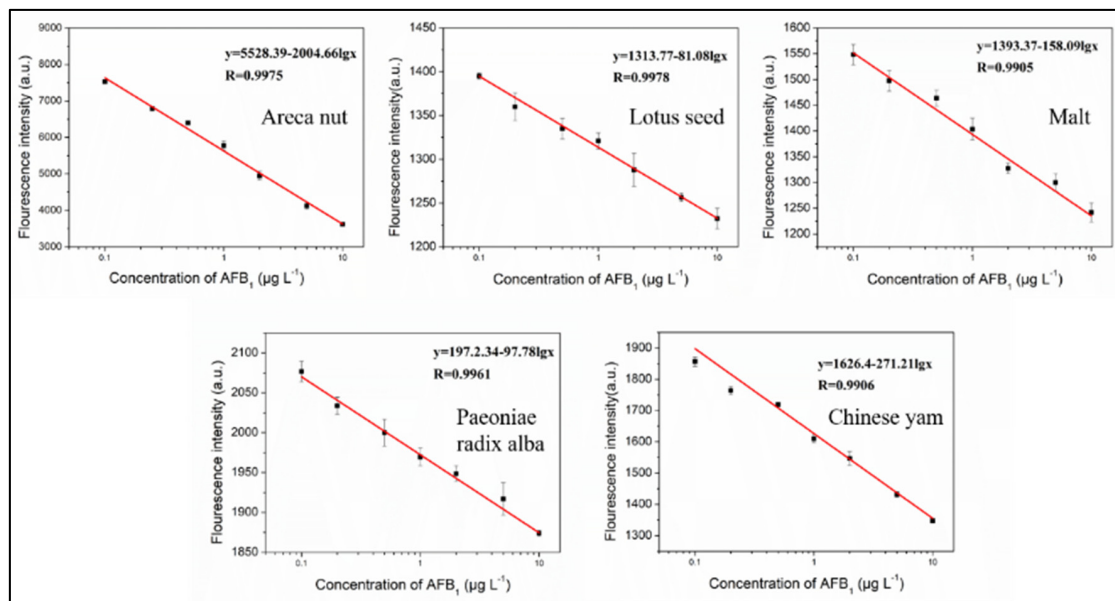


Figure 5. Calibration plot with relative fluorescence of PG/aptamer duplexes mixed with different concentrations of AFB₁ in five TCMs extracts. Results are from three independent experiments.

Table 2. Recoveries from five TCMs spiked with three concentrations of aflatoxin B₁.

Recovery (%)	Spiking Level ($\mu\text{g}\cdot\text{kg}^{-1}$) ($n = 3$)		
	2.5	5	10
Areca nut	71.1 (2.6%)	78.9 (9.1%)	79.9 (10.2%)
Lotus seed	82.4 (4.6%)	81.4 (10.2%)	95.4 (8.7%)
Malt	75.5 (5.9%)	78.5 (1.3%)	100.4 (8.4%)
Paeoniae alba radix	99.2 (7.2%)	100.9 (4.6%)	79.4 (6.4%)
Chinese yam	89.4 (3.4%)	88.7 (5.6%)	95.5 (9.0%)

2.6. Application to Real Samples

An edible and medicinal food, areca nut is widely distributed in Southern and Southeast Asia, including China, India, and the Philippines. Currently, it is commonly used as the main ingredient of many prescription TCMs, including to treat various gastrointestinal, parasitic, and edematous diseases, due to its wide spectrum of biological and pharmacological activities [36]. Lotus seed, which is widely used as food in China, is rich in protein, amino acids, unsaturated fatty acids, and minerals. This seed contains approximately 19.85% protein (dry weight) and has a well-balanced amino acid composition according to the Food and Agriculture Organization of the United Nations/World Health Organization with nutritive properties similar to soybean [37]. As reported in many studies, Chinese yam contains a variety of functional components, such as polysaccharides, choline, saponins, cholesterol, and phytic acid [38]. *Paeoniae alba Radix* is the *Ranunculaceae peony* root of *P. lactiflora* Pall. It has been used as an analgesic, sedative, and anti-inflammatory agent in Asia. It is also commonly used to treat patients with cardiovascular extravasated or stagnated blood [39]. However, this TCM is susceptible to toxigenic molds and the production of hazardous aflatoxin due to high temperatures and humidity where these TCMs are stored. Therefore, it is of great importance to routinely screen and measure aflatoxin contamination in TCMs prior to consumption.

The results of our study suggest our established method could be widely applicable in studies of complex medicinal herbs. To test the feasibility of our approach in real samples, five TCMs samples were collected from different regions and analyzed. As shown in Table 3, AFB₁ was detected in six batches of the twenty tested, where three contained levels exceeding the tolerable maximum level in

most foodstuffs of $5 \mu\text{g}\cdot\text{kg}^{-1}$. To confirm this result, the suspected samples were further analyzed by liquid chromatography-electrospray tandem mass spectrometry (Appendix A). These samples were verified as positive for AFB₁ based on two ion peaks in the extracts compared to AFB₁ standard. The above results indicate positive samples could be determined to be AFB₁ positive sensitively and accurately using the proposed method, demonstrating that this method is a promising rapid screening tool for AFB₁ contamination of TCMs.

Table 3. Aflatoxin B₁ contamination levels in samples.

	Samples	Aflatoxin B ₁ Contaminated Level ($\mu\text{g}\cdot\text{kg}^{-1}$)	RSD (%)
Areca nut	China (Guangxi province)	ND	-
	China (Hainan province)	<LOQ	-
	India	1.1	4.6
	Indonesia	58.1	7.2
	Philippines	97.1	6.4
Lotus seed	China (Hunan province)	63.2	5.7
	China (Hubei province)	ND	-
	China (Beijing province)	ND	-
	China (Fujian province)	ND	-
Malt	China (Hebei province)	ND	-
	China (Hebei province)	0.8	4.9
	China (Hebei province)	ND	-
	China (Hebei province)	ND	-
Paeoniae alba radix	China (Zhejiang province)	ND	-
	China (Anhui province)	ND	-
	China (Anhui province)	ND	-
	China (Anhui province)	ND	-
Chinese yam	China (Henan province)	ND	-
	China (Henan province)	ND	-
	China (Henan province)	ND	-
	China (Guangxi province)	ND	-

3. Conclusions

In summary, a simple and rapid aptamer-based label-free strategy was developed for highly selective and sensitive fluorescence detection of AFB₁ in complicated TCMs matrices. In view of the high selectivity of aptamer to AFB₁ and the ultra-sensitivity of PG for trace dsDNA, the proposed method accurately quantified nanomolar levels of AFB₁. Because TCMs have complex matrices that interfere with detection of specific components, this interference was overcome by dissolution in TE buffer and background correction, largely simplifying the process. The entire detection process could be completed in 30 min. Due to its simple, label-free design, fast response, and high selectivity, the proposed method is a significant improvement in AFB₁ screening during monitoring of TCM safety. Importantly, this is promising as a universal method due to the exceptional selectivity of PG for dsDNA and the potential extension of this principle to detecting other targets for which aptamers are available.

4. Materials and Methods

4.1. Reagents and Chemicals

Mycotoxin standards including AFB₁, AFM₁, OTA, ZEN, FB₁, and DON were purchased from Pribolab (Singapore, Singapore). A total of seven oligonucleotide sequences against AFB₁ and each corresponding complementary ssDNA were synthesized and purified through HPLC by Sangon Biotechnology Co., Ltd. (Shanghai, China), and these aptamers were listed in Table 1 and their corresponding complementary sequences (Seq) was listed in Table S1. The fluorescent dye PicoGreen was purchased from Invitrogen (Carlsbad, CA, USA). The areca nuts, lotus seed, malt, *Radix Paeoniae Alba*, and Chinese yam were collected from China, India, Philippines, and Indonesia.

Acetonitrile, methanol, Tris-HCl, EDTA-2Na, Na₂CO₃, NaHCO₃, and NaCl was analytical grade and purchased from Beijing Chemical Works (Beijing, China). PestiCarb (GCB 120-400 Mesh), octadecylsilane (C18) and Cleanert primary secondary amine (PSA, 40–60 µm) were from Beijing Agela Technologies Inc. Deionized water was purified using a Milli-Q system (Millipore, CA, USA).

4.2. Sample Preparation

AFB₁ was extracted from test samples using ultrasound-assisted solid-liquid extraction. Briefly, 5.0 g of each ground sample was weighed in a 50 mL centrifuge tube and 1.0 g NaCl and 25.0 mL of solvent consisting of acetonitrile/water (70/30, v/v) were added. The mixture was ultrasonicated in an ultrasonic clean bath at 500 W for 15 min and then centrifuged at 10,000 rpm for 5 min. For areca nuts, 2 mL of the supernatant was added to 0.25 g primary secondary amine(PSA), and 0.3 g graphitized carbon black(GCB). For other samples, 2 mL of supernatant was mixed with 0.25 g octadecylsilane (C18), vortexed for 2 min, and then centrifuged at 10,000 rpm for 5 min. For the areca nut samples, 1 mL supernatant was mixed with 150 µL of carbonate buffer solution (pH 9.6). This mixture was immediately transferred to a 2 mL tube and dried through evaporation under a stream of nitrogen gas at 40 °C. The residue was redissolved in TE buffer containing 10% methanol and centrifuged at 10,000 rpm for 5 min. The resulting supernatant was then used for fluorescent detection as described below.

4.3. Fluorescent Detection

For AFB₁ detection, the control and test groups were tested in parallel. In the test group, 25 µL of 20 mM AFB₁ specific-aptamer solution was mixed with 50 µL AFB₁ standard or sample solution dissolved in TE buffer in microplate wells. These mixtures were incubated at room temperature for 20 min. Next, 25 µL of 20 mM Seq and 10 µL of 10X PG were added to each well. After incubating for 5 min, the fluorescence intensities of the wells were recorded using a multifunction microplate reader (Tecan Infinite M1000, Tecan Austria GmbH, Grödig, Austria) with an excitation of 480 nm and emission of 520 nm. The control group was tested using the same procedure as for the test group except TE buffer or negative sample solution was used in place of standard solution. Each experimental condition was tested in triplicate. M1000

Supplementary Materials: The following are available online at www.mdpi.com/xxx/s1, Figure S1: Fluorescence intensity of aptamer binds with same length but different complementary sequence by various concentrations of AFB₁, Figure S2: Optimization of the addition amount of the PicoGreen were added into the aptamer and complementary strand mixture, Figure S3: Optimization of the incubation time after aptamer complementary strand and PicoGreen were added into the different concentration of AFB₁ and aptamer mixture, Figure S4: Calibration plot relative Fluorescence of the PG/aptamer duplex mixture against different concentrations of AFB₁ in arecae nut extract (black line, $y = 5528.39 - 2004.661gx$, $R = 0.9975$) and TE buffer (red line, $y = 5527.48 - 1976.131gx$, $R = 0.9987$), Table S1: DNA aptamer corresponding complementary sequence used in this study.

Acknowledgments: This work was supported by National Key R&D Program of China (2016YFE0112900), EU project H2020-E.U.3.2-678781-MycoKey, National Project for Standardization of Chinese Materia Medica (ZYBZH-Y-JIN-34), CAMS Innovation Fund for Medical Sciences (2016-I2M-1-012, 2017-I2M-1-013).

Author Contributions: Cheng Zhang and Xiaowen Dou conceived and designed the experiment; Cheng Zhang and Meifeng Sun performed the experiment; Cheng Zhang analyzed the data and wrote the manuscript; Lei Zhang assisted with the experiment and edited the manuscript; Ming Zhao, Zhen OuYang, Dandan Kong, F. Logrieco Antonio, and Meihua Yang supervised the researched, edited, and approved the final manuscript.

Conflicts of Interest: The authors declare no conflict of interest.

Appendix A

Ultra fast liquid chromatography (UFLC)-MS/MS analysis: Sample analysis was performed using an Applied Biosystems Sciex Qtrap[®]5500 MS/MS system (Foster, CA, USA) equipped with an electrospray ionization (ESI) source coupled with a UFLC system from Shimadzu (Kyoto, Japan). The Applied Biosystems Analyst software (version 1.6.2) was used to control the UFLC-MS/MS system and for data acquisition and processing. The mycotoxins were separated on a Shiseio Capcell Core C18 column (100 × 2.1 mm I.D., 2.7 µm; Shiseio, Japan). The mobile phase consisted of (A) acetonitrile

(0.1% formic acid) and (B) water (0.1% formic acid) at a flow rate of 0.3 mL·min⁻¹ and the injection volume was 2 µL. The optimized gradient elution procedure was as follows: 0~0.5 min, 10~30% A; 0.5~1 min, 30% A; 1~8 min, 30~95% A; 8~10 min, 95% A; 10.01~12 min, 10% A. The mass spectrometer was operated in the positive ESI mode with MRM at unit resolution. The main MS parameters were optimized and finally set as follows: nebulizer gas (GS1), 50 psi; auxiliary gas (GS2), 50 psi; curtain gas (CUR), 35 psi; capillary temperature, 550 °C; ion spray voltage (IS), +5500 V. Nitrogen was used as the nebulizer, heater, curtain, and collision gas. The precursor-to-product ion transitions were m/z 313.1/285.1 and m/z 313.1/245.0 for AFB₁, m/z 315.1/287.0 and m/z 315.1/259.0 for AFB₂, m/z 329.1/243.0 and m/z 329.1/311.2 for AFG₁, m/z 331.1/285.1 and m/z 331.1 / 241.0 for AFG₂.

References

1. Cancer, I.A.F.O. *Some Naturally Occurring Substances: Food Items and Constituents, Heterocyclic Aromatic Amines and Mycotoxins*; World Health Organization: Geneva, Switzerland, 1993.
2. Heather, S.; Eduardo, A.-B.; EMarianne, B.; Ramesh, V.B.; Robert, B.; Brune, M.N.; DeCock, K.; Dilley, A.; Groopman, J.; Hell, K. Workgroup report: Public health strategies for reducing aflatoxin exposure in developing countries. *Environ. Health Perspect.* **2006**, *114*, 1898–1903.
3. Kensler, T.W.; Roebuck, B.D.; Wogan, G.N.; Groopman, J.D. Aflatoxin: A 50-Year Odyssey of Mechanistic and Translational Toxicology. *Toxicol. Sci.* **2011**, *120* (Suppl. 1), S28–S48. [[CrossRef](#)] [[PubMed](#)]
4. Bbosa, G.S.; Kitya, D.; Odda, J.; Ogwalokeng, J. Aflatoxins metabolism, effects on epigenetic mechanisms and their role in carcinogenesis. *Health* **2013**, *5*, 14–34. [[CrossRef](#)]
5. Abdel-Aziem, S.H. Dietary supplementation with whey protein and ginseng extract counteracts oxidative stress and DNA damage in rats fed an aflatoxin-contaminated diet. *Mutat. Res.* **2011**, *723*, 65–71. [[CrossRef](#)] [[PubMed](#)]
6. Mary, V.S.; Theumer, M.G.; Arias, S.L.; Rubinstein, H.R. Reactive oxygen species sources and biomolecular oxidative damage induced by aflatoxin B1 and fumonisin B1 in rat spleen mononuclear cells. *Toxicology* **2012**, *302*, 299–307. [[CrossRef](#)] [[PubMed](#)]
7. Abbès, S.; Salah-Abbès, J.B.; Sharafi, H.; Jebali, R.; Noghabi, K.A.; Oueslati, R. Ability of *Lactobacillus rhamnosus* GAF01 to remove AFM1 in vitro and to counteract AFM1 immunotoxicity in vivo. *J. Immunotoxicol.* **2013**, *10*, 279–286. [[CrossRef](#)] [[PubMed](#)]
8. Fallah, A.A. Aflatoxin M1 contamination in dairy products marketed in Iran during winter and summer. *Food Control* **2010**, *21*, 1478–1481. [[CrossRef](#)]
9. Ji, E.L.; Kwak, B.M.; Ahn, J.H.; Jeon, T.H. Occurrence of aflatoxin M 1 in raw milk in South Korea using an immunoaffinity column and liquid chromatography. *Food Control* **2009**, *20*, 136–138.
10. Abia, W.A.; Warth, B.; Sulyok, M.; Krska, R.; Tchana, A.N.; Njobeh, P.B.; Dutton, M.F.; Moundipa, P.F. Determination of multi-mycotoxin occurrence in cereals, nuts and their products in Cameroon by liquid chromatography tandem mass spectrometry (LC-MS/MS). *Food Control* **2013**, *31*, 438–453. [[CrossRef](#)]
11. Li, M.; Kong, W.; Li, Y.; Liu, H.; Liu, Q.; Dou, X.; Ouyang, Z.; Yang, M. High-throughput determination of multi-mycotoxins in Chinese yam and related products by ultra fast liquid chromatography coupled with tandem mass spectrometry after one-step extraction. *J. Chromatogr. B* **2016**, *1022*, 118–125. [[CrossRef](#)] [[PubMed](#)]
12. Guan, D.; Li, P.; Zhang, Q.; Zhang, W.; Zhang, D.; Jiang, J. An ultra-sensitive monoclonal antibody-based competitive enzyme immunoassay for aflatoxin M₁ in milk and infant milk products. *Food Chem.* **2011**, *125*, 1359–1364. [[CrossRef](#)]
13. Bradburn, N.; Coker, R.D.; Blunden, G. A comparative study of solvent extraction efficiency and the performance of immunoaffinity and solid phase columns on the determination of aflatoxin B 1. *Food Chem.* **1995**, *52*, 179–185. [[CrossRef](#)]
14. Romagnoli, B.; Menna, V.; Gruppioni, N.; Bergamini, C. Aflatoxins in spices, aromatic herbs, herb-teas and medicinal plants marketed in Italy. *Food Control* **2007**, *18*, 697–701. [[CrossRef](#)]
15. Nonaka, Y.; Saito, K.; Hanioka, N.; Narimatsu, S.; Kataoka, H. Determination of aflatoxins in food samples by automated on-line in-tube solid-phase microextraction coupled with liquid chromatography-mass spectrometry. *J. Chromatogr. A* **2009**, *1216*, 4416–4422. [[CrossRef](#)] [[PubMed](#)]

16. Zhao, M.; Zhuo, Y.; Chai, Y.; Xiang, Y.; Liao, N.; Gui, G.; Yuan, R. Dual signal amplification strategy for the fabrication of an ultrasensitive electrochemiluminescent aptasensor. *Analyst* **2013**, *138*, 6639–6644. [[CrossRef](#)] [[PubMed](#)]
17. Tuerk, C.; Gold, L. Systematic evolution of ligands by exponential enrichment: RNA ligands to bacteriophage T4 DNA polymerase. *Science* **1990**, *249*, 505–510. [[CrossRef](#)] [[PubMed](#)]
18. Ellington, A.D.; Szostak, J.W. Selection in vitro of single-stranded DNA molecules that fold into specific ligand-binding structures. *Nature* **1992**, *355*, 850–852. [[CrossRef](#)] [[PubMed](#)]
19. Mayer, G. The chemical biology of aptamers. *Angew. Chem. Int. Ed. Engl.* **2009**, *48*, 2672–2689. [[CrossRef](#)] [[PubMed](#)]
20. Liu, J.; Guan, Z.; Lv, Z.; Jiang, X.; Yang, S.; Chen, A. Improving sensitivity of gold nanoparticle based fluorescence quenching and colorimetric aptasensor by using water resuspended gold nanoparticle. *Biosens. Bioelectron.* **2014**, *52*, 265–270. [[CrossRef](#)] [[PubMed](#)]
21. Bonel, L.; Vidal, J.C.; Duato, P.; Castillo, J.R. An electrochemical competitive biosensor for ochratoxin A based on a DNA biotinylated aptamer. *Biosens. Bioelectron.* **2011**, *26*, 3254–3259. [[CrossRef](#)] [[PubMed](#)]
22. Cruzaguado, J.A.; Penner, G. Fluorescence Polarization Based Displacement Assay for the Determination of Small Molecules with Aptamers. *Anal. Chem.* **2008**, *80*, 8853–8855. [[CrossRef](#)] [[PubMed](#)]
23. Kuang, H.; Chen, W.; Xu, D.; Xu, L.; Zhu, Y.; Liu, L.; Chu, H.; Peng, C.; Xu, C.; Zhu, S. Fabricated aptamer-based electrochemical “signal-off” sensor of ochratoxin A. *Biosens. Bioelectron.* **2010**, *26*, 710–716. [[CrossRef](#)] [[PubMed](#)]
24. Sheng, L.; Ren, J.; Miao, Y.; Wang, J.; Wang, E. PVP-coated graphene oxide for selective determination of ochratoxin A via quenching fluorescence of free aptamer. *Biosens. Bioelectron.* **2011**, *26*, 3494–3499. [[CrossRef](#)] [[PubMed](#)]
25. Castillo, G.; Lamberti, I.; Mosiello, L.; Hianik, T. Impedimetric DNA Aptasensor for Sensitive Detection of Ochratoxin A in Food. *Electroanalysis* **2012**, *24*, 512–520. [[CrossRef](#)]
26. Galarreta, B.C.; Tabatabaei, M.; Guieu, V.; Peyrin, E.; Lagugn e-Labarthe, F. Microfluidic channel with embedded SERS 2D platform for the aptamer detection of ochratoxin A. *Anal. Bioanal. Chem.* **2013**, *405*, 1613–1621. [[CrossRef](#)] [[PubMed](#)]
27. Zhang, J.; Zhang, X.; Yang, G.; Chen, J.; Wang, S. A signal-on fluorescent aptasensor based on Tb³⁺ and structure-switching aptamer for label-free detection of Ochratoxin A in wheat. *Biosens. Bioelectron.* **2013**, *41*, 704–709. [[CrossRef](#)] [[PubMed](#)]
28. Dragan, A.I.; Bishop, E.S.; Casas-Finet, J.R.; Strouse, R.J.; Schenerman, M.A.; Geddes, C.D. Metal-enhanced PicoGreen[®] fluorescence: Application to fast and ultra-sensitive pg/mL DNA quantitation. *J. Immunol. Methods* **2010**, *362*, 95–100. [[CrossRef](#)] [[PubMed](#)]
29. Singer, V.L.; Jones, L.J.; Yue, S.T.; Haugland, R.P. Characterization of PicoGreen reagent and development of a fluorescence-based solution assay for double-stranded DNA quantitation. *Anal. Biochem.* **1997**, *249*, 228–238. [[CrossRef](#)] [[PubMed](#)]
30. Ma, X.; Wang, W.; Chen, X.; Xia, Y.; Wu, S.; Duan, N.; Wang, Z. Selection, identification, and application of Aflatoxin B1 aptamer. *Eur. Food Res. Technol.* **2014**, *238*, 919–925. [[CrossRef](#)]
31. Le, L.C.; Cruz-Aguado, J.A.; Penner, G.A. DNA Ligands for Aflatoxin and Zearalenone. U.S. Patent EP20100809412, 24 February 2011.
32. Shim, W.B.; Mun, H.; Joung, H.A.; Ofori, J.A.; Chung, D.H.; Kim, M.G. Chemiluminescence competitive aptamer assay for the detection of aflatoxin B1 in corn samples. *Food Control* **2014**, *36*, 30–35. [[CrossRef](#)]
33. Zhu, Z.; Song, Y.; Li, C.; Zou, Y.; Zhu, L.; An, Y.; Yang, C.J. Monoclonal surface display SELEX for simple, rapid, efficient, and cost-effective aptamer enrichment and identification. *Anal. Chem.* **2014**, *86*, 5881–5888. [[CrossRef](#)] [[PubMed](#)]
34. Wu, S.Q.; Yang, M.Z.; Zhang, L. Aflatoxin B1 Nucleic Acid Aptamers and Their Applications. C.N. Patent 120517289A, 27 June 2012.
35. Liao, Q.; Luo, G.L.; Li, W.; Hu, L. Preparation Method of Aflatoxin B1 Aptamer Affinity Column. C.N. Patent 104399283A, 11 March 2015.
36. Chavan, Y.; Singhal, R.S. Ultrasound-assisted extraction (UAE) of bioactives from arecanut (*Areca catechu* L.) and optimization study using response surface methodology. *Innov. Food Sci. Emerg. Technol.* **2013**, *17*, 106–113. [[CrossRef](#)]

37. Zeng, H.Y.; Cai, L.H.; Cai, X.L.; Wang, Y.J.; Li, Y.Q. Amino acid profiles and quality from lotus seed proteins. *J. Sci. Food Agric.* **2013**, *93*, 1070–1075. [[CrossRef](#)] [[PubMed](#)]
38. Ju, Y.; Xue, Y.; Huang, J.; Zhai, Q.; Wang, X.H. Antioxidant Chinese yam polysaccharides and its pro-proliferative effect on endometrial epithelial cells. *Int. J. Biol. Macromol.* **2014**, *66*, 81–85. [[CrossRef](#)] [[PubMed](#)]
39. Qiu, Z.K.; He, J.L.; Liu, X.; Zeng, J.; Chen, J.S.; Nie, H. Anti-PTSD-like effects of albiflorin extracted from *Radix paeoniae Alba*. *J. Ethnopharmacol.* **2017**, *198*, 324–330. [[CrossRef](#)] [[PubMed](#)]



© 2018 by the authors. Licensee MDPI, Basel, Switzerland. This article is an open access article distributed under the terms and conditions of the Creative Commons Attribution (CC BY) license (<http://creativecommons.org/licenses/by/4.0/>).